REPORT

NEUROSCIENCE

Overlapping memory trace indispensable for linking, but not recalling, individual memories

Jun Yokose,[1,2] Reiko Okubo-Suzuki,[1,2] Masanori Nomoto,[1,2] Noriaki Ohkawa,[1,2]* Hirofumi Nishizono,[2,3] Akinobu Suzuki,[1,2] Mina Matsuo,[3] Shuhei Tsujimura,[1,2] Yukari Takahashi,[4] Masashi Nagase,[4] Ayako M. Watabe,[4] Masakiyo Sasahara,[5] Fusao Kato,[4] Kaoru Inokuchi[1,2]†

Memories are not stored in isolation from other memories but are integrated into associative networks. However, the mechanisms underlying memory association remain elusive. Using two amygdala-dependent behavioral paradigms—conditioned taste aversion (CTA) and auditory-cued fear conditioning (AFC)—in mice, we found that presenting the conditioned stimulus used for the CTA task triggered the conditioned response of the AFC task after natural coreactivation of the memories. This was accompanied through an increase in the overlapping neuronal ensemble in the basolateral amygdala. Silencing of the overlapping ensemble suppressed CTA retrieval-induced freezing. However, retrieval of the original CTA or AFC memory was not affected. A small population of coshared neurons thus mediates the link between memories. They are not necessary for recalling individual memories.

Memories are often stored in interconnected networks of the brain to associate with one another (*1*–*5*). The simultaneous retrieval of two independent memories sometimes links the original memories, generating a qualitatively new memory. Memory is encoded in a specific cell ensemble that is activated during learning (*6*–*9*), and individual memories are generally represented by different cell ensembles. Acquisition of a new memory can be modified by the simultaneous and artificial reactivation of a specific neuronal ensemble corresponding to that prestored memory, generating synthetic or false memories (*10*, *11*). When an association is formed between conditioned and unconditioned stimuli (CS and US, respectively) in Pavlovian conditioning, cell ensembles corresponding to each stimulus overlap, and this is thought to link these stimuli (*4*, *12*–*14*). We investigated the nature of these overlapping neuronal ensembles in the association of memories governed by repeated and simultaneous retrieval.

Mice were trained independently on two behavioral tasks: conditioned taste aversion (CTA) on days 5 and 6 and auditory-cued fear conditioning (AFC) on day 10 (Fig. 1A). After each memory was formed, animals received synchronous and repetitive copresentations of the CS for CTA (saccharin solution as CS1) and that for AFC (tone as CS2) during repeated coretrieval sessions (RCSs) in which the tone was presented as soon as mice licked the nozzle that provides the saccharin solution. The CTA and AFC memories in these mice were comparable with those in control animals throughout the entire session, which did not receive the CS2 (tone) during the RCS (Fig. 1, B and C). After the RCS, within the first several minutes of licking the saccharin solution during the subsequent CTA test, mice in the coretrieval group showed a long latency to move from the corner of the CTA chamber, decreased mobility, and freezing behavior (test 1) (Fig. 1, D to F, and fig. S1). Thus, CS1 (saccharin) triggered a freezing response after the RCS (saccharin-induced freezing). Mice in the unpaired group, which received CS1 and CS2 at 30-min intertrial intervals during the RCS, showed freezing behavior upon saccharin-licking comparable with that in the coretrieval group (fig. S2, A to D). Thus, a group of mice that received only CS1 during the RCS served as a control group. The link between CS1 and CS2 was not formed without acquiring the CTA memory (fig. S2, E to H) and did not depend on the order of the training (fig. S2, I to L).

We analyzed c-Fos expression as a marker of neuronal activity in brain areas shown to be important for the performance of CTA and AFC, including the basolateral amygdala, medial prefrontal cortex, and insular cortex (*13*–*21*). The number of c-Fos–positive cells in the basolateral amygdala was significantly higher in the coretrieval group than in the control group (fig. S3).

Disrupting the CTA memory in mice subjected to the RCS rendered the AFC memory labile (Fig. 1, G to K) (*22*). We infused either the protein synthesis inhibitor anisomycin or vehicle bilaterally into the basolateral amygdala of mice immediately after the CTA retrieval test (test 1) that followed the RCS (Fig. 1G). Retention of the CTA memory was disrupted in the anisomycin group compared with control (Fig. 1H). This disruption was accompanied by an impairment in the original AFC memory, although the AFC memory had not been directly reactivated during the anisomycin infusion (Fig. 1I). A second nonreactivated group of mice that had not received the RCS (no RCS, home cage group) also showed the CTA memory impairment, but their AFC memory recall was intact (Fig. 1, J and K).

Cellular compartment analysis of temporal activity by use of fluorescence in situ hybridization with Arc and Homer 1a (Arc/H1a catFISH) (*23*, *24*) revealed a dynamic interaction between CTA and AFC at the neuronal ensemble level in all the brain areas analyzed (Fig. 2 and fig. S4). The population of the Arc/H1a–double-positive neurons in the basolateral amygdala of the coretrieval group was significantly greater than that in the control and no-reactivation groups, despite the same-sized population of Arc/H1a–single-positive cells among the groups (Fig. 2, B to E, and fig. S4). The percentage of the coshared neuronal population (overlapping ensemble) in the amygdala between CTA and AFC to the total ensembles activated during retrieval was 15.2% for the coretrieval, 9.1% for the control, and 8.2% for the no-reactivation groups (Fig. 2F).

Coactivity of specific subsets of neurons triggers the association of memories (*12*, *25*). To test whether ensemble coactivity during RCS is critical for the CTA-AFC interaction, we used optogenetic manipulation to suppress the AFC ensemble activity in the basolateral amygdala during RCS. We applied to c-fos–tetracycline (tet)–controlled transactivator (tTA) transgenic mice (*26*) a tet-OFF lentiviral vector encoding enhanced archaerhodopsin-T 3.0 fused to enhanced yellow fluorescent protein (ArchT-EYFP) (Fig. 3, A to C) (*4*). ArchT-EYFP labeled the AFC training ensemble in a doxycycline (Dox)– and AFC training–dependent manner (fig. S5). We then examined, ex vivo and in vivo, whether optical stimulation suppressed the activity of the neuronal ensemble that had been labeled during the AFC training. In ex vivo patch-clamp recordings with yellow-light illumination, ArchT-EYFP-expressing, but not EYFP-expressing, cells elicited a robust and sustained hyperpolarizing current that effectively blocked action potentials evoked by somatic current injections (Fig. 3, D and E, and fig. S6, A and B). Spontaneous activity was

[1]Department of Biochemistry, Faculty of Medicine, Graduate School of Medicine and Pharmaceutical Sciences, University of Toyama, 2630 Sugitani, Toyama 930-0194, Japan. [2]Core Research for Evolutional Science and Technology (CREST), Japan Science and Technology Agency (JST), University of Toyama, 2630 Sugitani, Toyama 930-0194, Japan. [3]Division of Animal Experimental Laboratory, Life Science Research Centre, University of Toyama, 2630 Sugitani, Toyama 930-0194, Japan. [4]Department of Neuroscience, Jikei University School of Medicine, Tokyo 105-8461, Japan. [5]Department of Pathology, Faculty of Medicine, University of Toyama, 2630 Sugitani, Toyama 930-0194, Japan.
*Present address: Precursory Research for Embryonic Science and Technology (PRESTO), JST, University of Toyama, 2630 Sugitani, Toyama 930-0194, Japan. †Corresponding author. Email: inokuchi@med.u-toyama.ac.jp

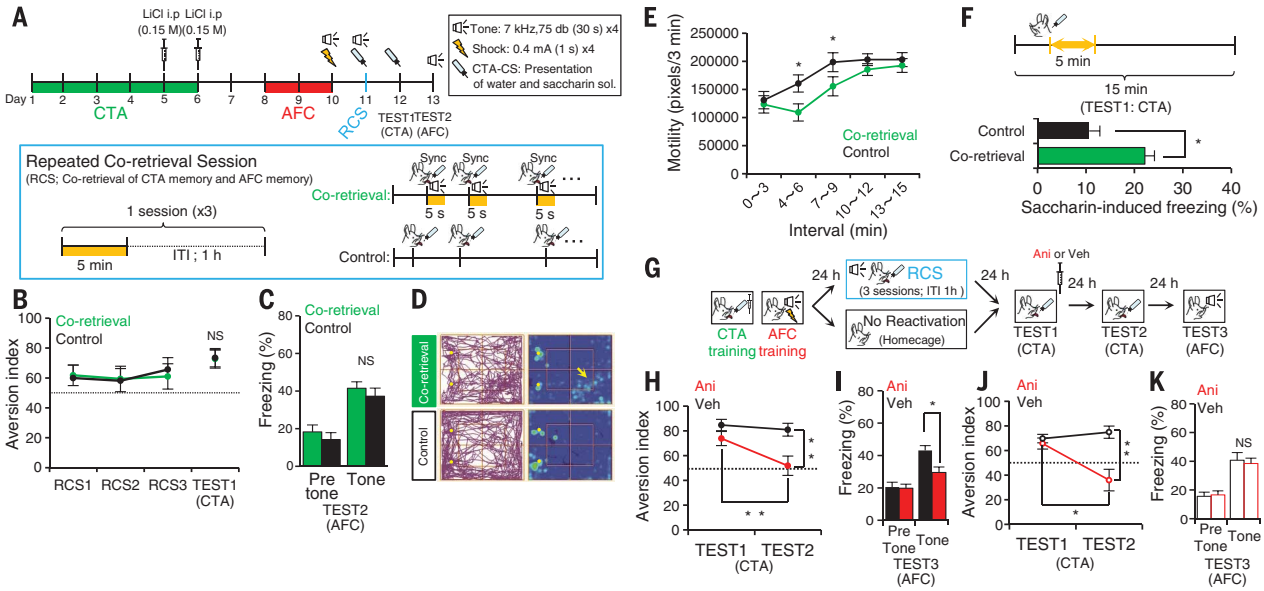

Fig. 1. Saccharin-induced freezing is generated through repetitive memory retrieval. (**A**) Experimental design. (**B** and **C**) Original CTA (B) and AFC memories (C) examined after the RCS. Aversion index for CTA memory performance in the RCS and test 1 [*t* test, $n = 12$ mice, $P > 0.19$ (not significant, *N.S.*), $t_{22} = 1.35$]. Freezing (%) in test 2 (*t* test, $n = 12$ mice, $P > 0.42$, $t_{22} = 0.81$). (**D**) Behavioral tracing (left) and occupancy plots (right) during test 1. Yellow arrow shows longer latency to move from the corner in the coretrieval group. The solid yellow circles indicate the nozzle positions for water and saccharin. (**E**) Mouse motility examined in 3-min intervals during test 1. Two-way analysis of variance (ANOVA), $P > 0.23$, $F_{4,119} = 1.42$; Wilcoxon rank-sum test 4 to 6 min, $P = 0.012$, $z = -2.51$; 7 to 9 min, $P = 0.04$, $z = -2.04$. (**F**) Saccharin-induced freezing (%) measured for 5 min (yellow bar) immediately after finishing licking saccharin in test 1 (*t* test, $n = 12$ mice, $P = 0.04$, $t_{22} = 2.23$). (**G**) Behavioral testing schedule for examining the link between CTA and AFC memories. Anisomycin (Ani) or vehicle (Veh) was bilaterally infused in the BLA immediately after the CTA retrieval test (test 1). (**H** and **I**) RCS group. Aversion index in test 1 and test 2 [*t* test; test 1 versus test 2 in Ani group, $n = 12$ mice, $P = 0.0075$, $t_{11} = 3.27$; Ani ($n = 12$ mice) versus Veh ($n = 13$ mice) in test 2, $P = 0.0015$, $t_{23} = 3.59$], and freezing (%) in test 3 (*t* test, $P = 0.013$, $t_{23} = 2.68$). (**J** and **K**) No RCS group. Aversion index in test 1 and test 2 [*t* test; test 1 versus test 2 in Ani, $n = 10$ mice, $P = 0.015$, $t_9 = 3.01$; coretrieval group ($n = 10$ mice) versus control ($n = 11$ mice) in test 2, $P = 0.0008$, $t_{19} = 3.96$], and freezing (%) in test 3 (*t* test, $P > 0.74$, $t_{19} = 0.33$). Data are means ± SEM. Significance for multiple comparisons, $^*P < 0.05$, $^{**}P < 0.01$.

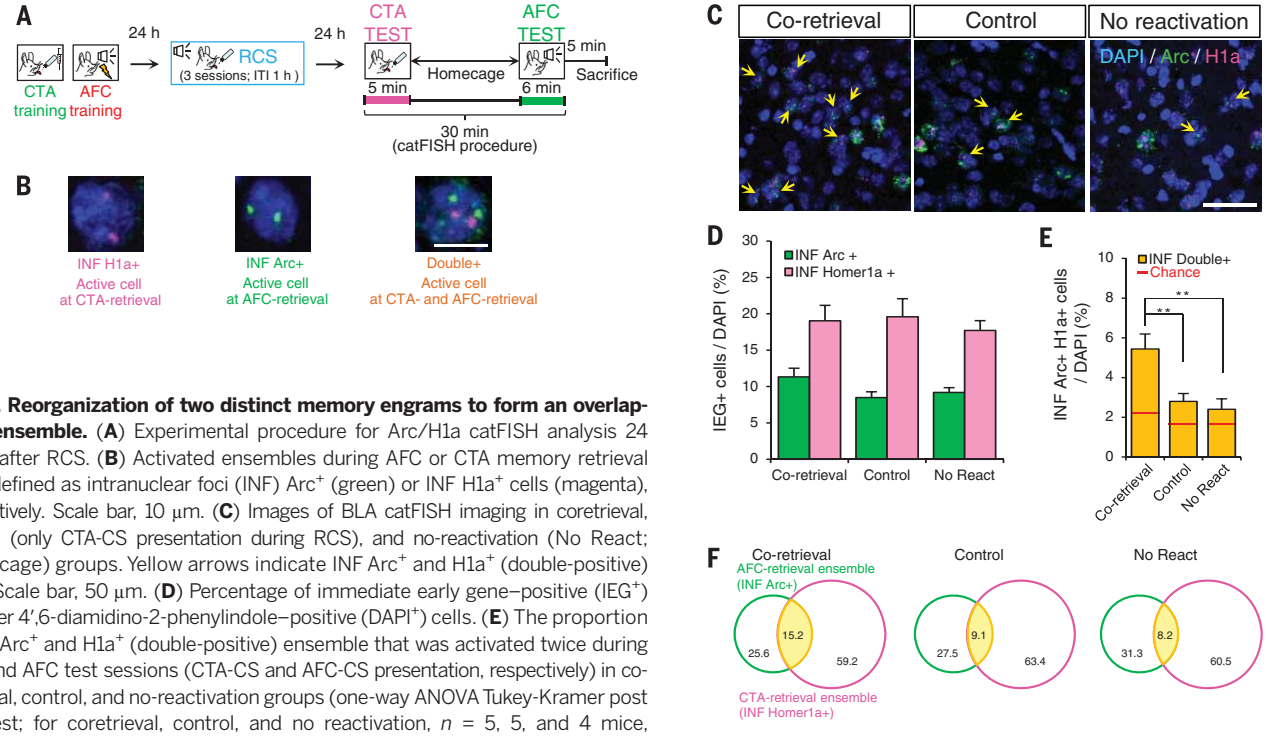

Fig. 2. Reorganization of two distinct memory engrams to form an overlapping ensemble. (**A**) Experimental procedure for Arc/H1a catFISH analysis 24 hours after RCS. (**B**) Activated ensembles during AFC or CTA memory retrieval were defined as intranuclear foci (INF) Arc^+ (green) or INF $H1a^+$ cells (magenta), respectively. Scale bar, 10 μm. (**C**) Images of BLA catFISH imaging in coretrieval, control (only CTA-CS presentation during RCS), and no-reactivation (No React; home cage) groups. Yellow arrows indicate INF Arc^+ and $H1a^+$ (double-positive) cells. Scale bar, 50 μm. (**D**) Percentage of immediate early gene–positive (IEG^+) cells per 4′,6-diamidino-2-phenylindole–positive ($DAPI^+$) cells. (**E**) The proportion of the Arc^+ and $H1a^+$ (double-positive) ensemble that was activated twice during CTA and AFC test sessions (CTA-CS and AFC-CS presentation, respectively) in coretrieval, control, and no-reactivation groups (one-way ANOVA Tukey-Kramer post hoc test; for coretrieval, control, and no reactivation, $n = 5$, 5, and 4 mice, respectively; $P = 0.0012$; $F_{2,13} = 23.07$). Red line indicates chance. (**F**) Scaled Venn diagrams representing the size and proportion of overlap in the activated ensembles of the BLA. Circle size reflects cell number, and numbers within the diagrams indicate the percentage contributed by each ensemble and the overlap. Data are means ± SEM. Significance for multiple comparisons, $^{**}P < 0.01$.

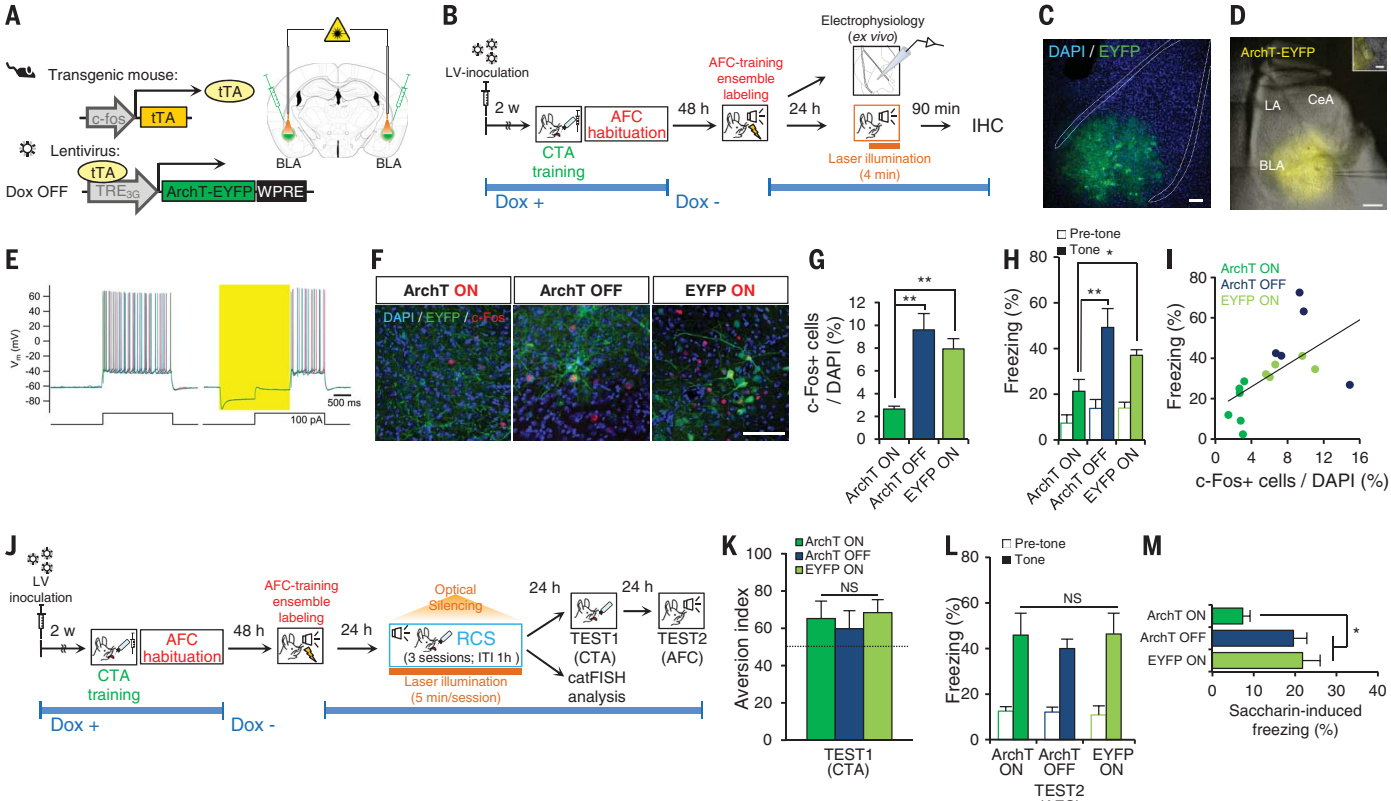

Fig. 3. Coactivity of distinct neuronal ensembles during the RCS generates a link between CTA and AFC memory. (**A**) Strategy to label the BLA AFC training ensemble. (**B**) Optical silencing of the neuronal ensemble induced by AFC training shown by electrophysiological slice recording ex vivo and c-Fos immunostaining in vivo. (**C**) BLA ArchT-EYFP–expressing cells (green) 24 hours after AFC training under OFF-Dox. The white dotted line indicates outline of amygdala. Scale bar, 100 μm. (**D**) Overlaid image of the oblique trans-illumination (monochrome) and the EYFP fluorescence (yellow) of a slice expressing ArchT-EYFP. The recorded neuron shows yellow fluorescence (inset). Scale bars, 200 μm; inset, 10 μm. (**E**) Membrane potentials (top) and the injected current (bottom) without (left) and with (right) yellow-light illumination (indicated with a yellow box) of a neuron expressing ArchT-EYFP in the BLA of a c-Fos::tTA mouse injected with LV. Depolarizing currents, 100 pA. Shown are overlaid traces of four consecutive sweeps with the same protocol. (**F**) c-Fos expression (red) 90 min after the AFC test. ON, laser illumination; OFF, no laser illumination. Scale bar, 100 μm. (**G**) Proportion of c-Fos$^+$ cells in each group (one-way ANOVA Tukey-Kramer post hoc test; for ArchT ON, ArchT OFF, and EYFP OFF, n = 6, 5, 5 mice, respectively; P = 0.0055; $F_{2,15}$ = 14.11). (**H**) Tone-induced freezing (%) under light illumination (one-way ANOVA Tukey-Kramer post hoc test; P = 0.0024, $F_{2,15}$ = 9.90). (**I**) Correlation between the percentage of c-Fos$^+$ cells and freezing (%) (Spearman's rank correlation coefficient, P = 0.012, rs = 0.65, z = 2.51). (**J**) Experimental procedure for disrupting ensemble activity during RCS by means of optical silencing. (**K** and **L**) Aversion index in test 1 for original CTA memory (one-way ANOVA, P > 0.89, $F_{2,19}$ = 0.12) and freezing (%) (one-way ANOVA, P > 0.81, $F_{2,19}$ = 0.21) in test 2 for original AFC memory (for ArchT ON, ArchT OFF, and EYFP OFF, n = 6, 8, and 6 mice, respectively). (**M**) Saccharin-induced freezing (%) measured for 5 min immediately after finishing the first lick of the saccharin nozzle during test 1 (one-way ANOVA Tukey-Kramer post hoc test, P = 0.0067, $F_{2,19}$ = 6.82). (**N** and **O**) The proportion of IEG$^+$ ensembles and the ratio of overlapping ensembles determined with catFISH staining 24 hours after light illumination (ArchT ON, ArchT OFF, EYFP ON, n = 7, 7, 6 mice, respectively; one-way ANOVA Tukey-Kramer post hoc test, P = 0.00017, $F_{2,19}$ = 15.08). Red line indicates chance. Data are means ± SEM. Significance for multiple comparisons, *P < 0.05, **P < 0.01.

suppressed with continuous optical stimulation for 5 min, with the firing properties subsequently recovering within several minutes (fig. S6, C and D). In vivo, optical silencing of the AFC training ensemble (ArchT laser ON group) significantly reduced the percentage of c-Fos$^+$ cells and tone-induced freezing compared with those in the ArchT laser OFF (ArchT OFF) and EYFP laser ON groups (EYFP ON) (Fig. 3, F to H). The magnitude of freezing correlated well with the number of c-Fos$^+$ cells (Fig. 3I).

We then applied tet-tagged optical silencing to mice subjected to RCS (Fig. 3J). ArchT-EYFP– or EYFP-tagged mice, whose basolateral amygdala cells were labeled during AFC training, received continuous light illumination during each of three RCSs. Optical silencing during RCS had no effect on the retrieval of the original CTA and AFC memories (Fig. 3, K and L). However, the percentage of saccharin-induced freezing during test 1 was significantly attenuated in the ArchT ON group as compared with the other groups (Fig. 3M). In catFISH imaging analysis conducted 24 hours after RCS (Fig. 3J), the number of Arc– or H1a–single-positive cells was similar in each group. However, the overlapping ensemble ratio in the ArchT ON group was significantly reduced as compared with that in the other groups (Fig. 3, N and O). Therefore, artificial disruption of the AFC training ensemble activity during RCS led to a decrease in the proportion of the overlapping neuronal ensemble and impaired the saccharin-induced freezing behavior.

Our findings raise a critical question: Does the neuronal activity of the overlapping ensemble in the basolateral amygdala mediate the cross-modal association that leads to saccharin-induced freezing? We developed a c-fos tTA-tet tag (*26*) and lentivirus-based genetic targeting system in combination with a tamoxifen-inducible Cre-loxP recombination system (*27*) that enabled us to specifically target the overlapping ensemble

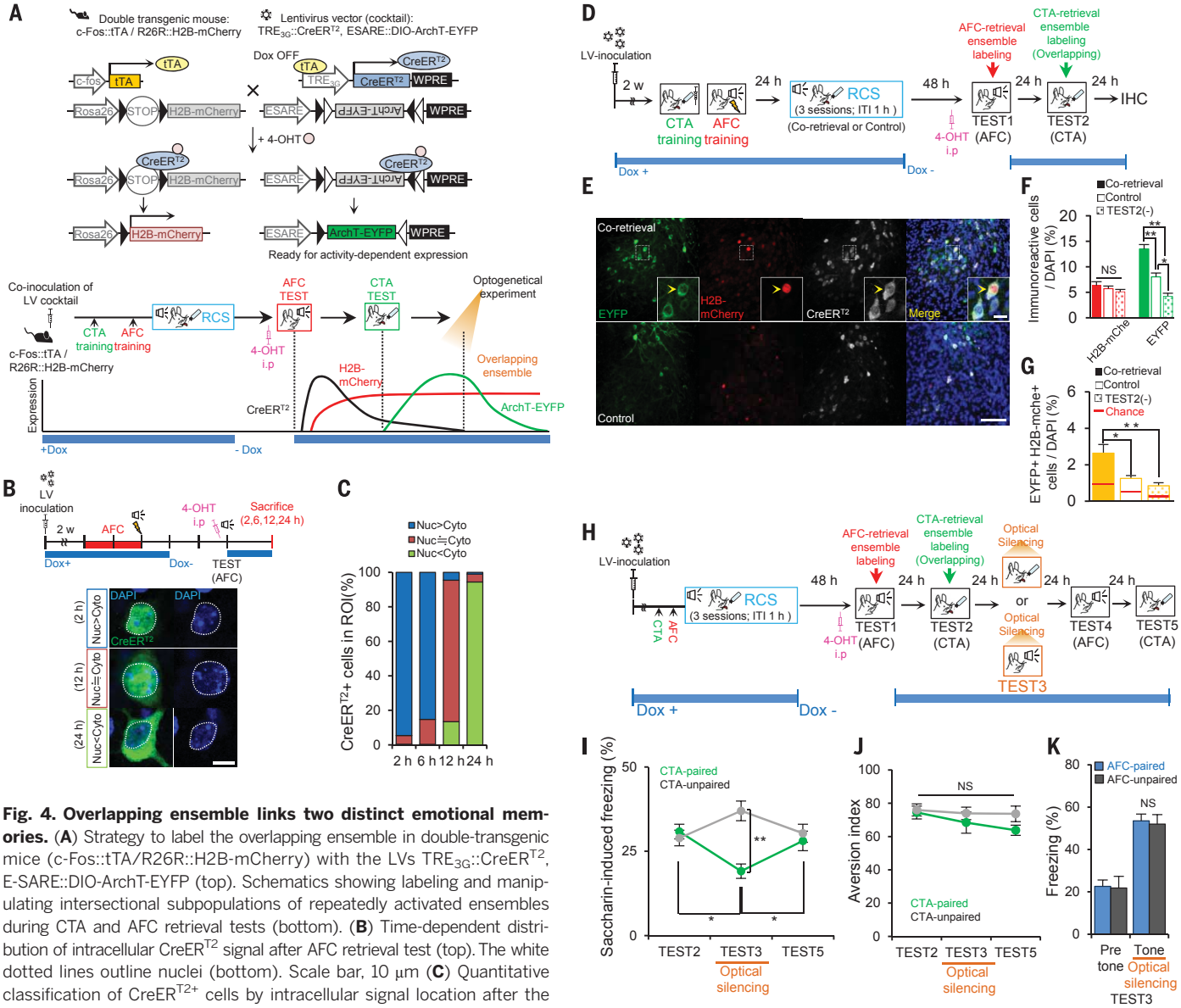

Fig. 4. Overlapping ensemble links two distinct emotional memories. (**A**) Strategy to label the overlapping ensemble in double-transgenic mice (c-Fos::tTA/R26R::H2B-mCherry) with the LVs TRE_{3G}::$CreER^{T2}$, E-SARE::DIO-ArchT-EYFP (top). Schematics showing labeling and manipulating intersectional subpopulations of repeatedly activated ensembles during CTA and AFC retrieval tests (bottom). (**B**) Time-dependent distribution of intracellular $CreER^{T2}$ signal after AFC retrieval test (top). The white dotted lines outline nuclei (bottom). Scale bar, 10 μm (**C**) Quantitative classification of $CreER^{T2+}$ cells by intracellular signal location after the AFC retrieval test. (**D**) Procedure for targeting the overlapping ensemble with ArchT-EYFP. (**E**) Overlapping ensembles expressing the ArchT-EYFP in coretrieval and control groups. Control group received only CTA-CS presentation during RCS. The yellow arrowheads indicate an ArchT-EYFP$^+$, H2B-mCherry$^+$ (double-positive) cell in the overlapping ensemble (insets). Scale bar, 100 μm; inset, 20 μm. (**F** and **G**) Quantitative population analysis of ArchT-EYFP$^+$ cells and mCherry$^+$ cells (F) and ArchT-EYFP$^+$, H2B-mCherry$^+$ (double-positive) cells (G). Coretrieval, control, test 2(−), n = 5, 4, 5 mice, respectively; H2B-mCherry$^+$, $P > 0.36$, $F_{2,13} = 1.13$; ArchT-EYFP$^+$, P = 7.44E-5, $F_{2,13} = 25.47$; ArchT-EYFP$^+$, H2B-mCherry$^+$, $P = 0.001$, $F_{2,13} = 13.36$. Red line indicates chance. (**H**) Procedure for suppressing the neuronal activity of the overlapping ensemble through yellow-light illumination. Mice received the same treatment until test 2 in (D). (**I**) Saccharin-induced freezing (%) during test 2, test 3 with light illumination, and test 5 (CTA-paired and CTA-unpaired, n = 13 and 12 mice, respectively; two-way ANOVA, Tukey-Kramer post hoc test, $P = 0.00051$, $F_{2,74} = 8.49$). (**J**) Aversion index in test 2, test 3, and test 5 of CTA-paired and CTA-unpaired groups (two-way ANOVA, $P > 0.64$, $F_{2,74} = 0.45$). (**K**) Tone-induced freezing (%) of AFC-paired and AFC-unpaired groups with light illumination in the AFC retrieval test (test 3) (AFC-paired, n = 8 mice; AFC-unpaired, n = 7 mice; t test, $P > 0.78$, $t_{13} = 0.28$). Data are means ± SEM. Significance for multiple comparisons, *$P < 0.05$, **$P < 0.01$.

(Fig. 4A). In a first step, the AFC retrieval ensemble was labeled with $CreER^{T2}$ under OFF-Dox conditions. In a second step, DIO-ArchT-EYFP under the control of the enhanced synaptic activity–responsive element (E-SARE) promoter (*28*) was transcribed in the cells of the CTA retrieval ensemble. Last, ArchT-EYFP protein was translated specifically in those cells that were activated twice, once during the AFC retrieval and again during the CTA retrieval—that is, in the cells of the overlapping ensemble.

The time-dependent change in the intracellular localization of CreERT2 was examined to determine the appropriate interval between the AFC and CTA tests (Fig. 4, B and C). Five hours before the AFC test under OFF-Dox conditions, 4-hydroxytamoxifen (4-OHT) was administered. $CreER^{T2}$ signals initially localized in the nucleus are translocated to the cytoplasm (*27*). This signal was detected exclusively in the cytoplasm 24 hours after the AFC retrieval test. Thus, Cre recombination hardly occurs at 24 hours or later, indicating that the interval between the AFC and CTA tests should be at least 24 hours.

Our immunohistochemical analysis revealed an increase in the number of ArchT-EYFP–positive cells in the coretrieval group, as compared with

the control group or the group that did not receive test 2 [test 2(−)] (13.5 ± 1.5%, 8.0 ± 1.2%, and 4.2 ± 1.0%, respectively) (Fig. 4, D to F). Thus, the increase depended on the RCS and the CTA retrieval at test 2. Moreover, the increase was consistent with that observed for the catFISH results (Fig. 2E), indicating that the overlapping population of cells was specifically labeled with ArchT-EYFP. We found no significant differences among groups for the number of H2B-mCherry$^+$ cells (Fig. 4F), which represent the AFC retrieval ensemble, thus showing an equivalent efficiency in Cre-mediated recombination. The number of ArchT$^+$, H2B-mCherry$^+$ (double-positive) cells in the coretrieval group was also significantly higher than in the control and test 2(−) groups (Fig. 4G).

Last, we investigated a causal relationship between the neuronal activity of the overlapping ensemble during RCS and the association between the CTA and AFC memories (Fig. 4, H to K). Animals labeled with ArchT-EYFP in the overlapping ensemble in the basolateral amygdala were divided into four groups that received the same treatments throughout the experiments, except during test 3 (Fig. 4H). Two groups were subjected to the CTA retrieval test with or without optical silencing (CTA-paired or CTA-unpaired, respectively). The other two groups were subjected to the AFC retrieval test with or without optical silencing (AFC-paired or AFC-unpaired, respectively). Optical silencing of the overlapping ensemble suppressed saccharin-induced freezing in test 3 (Fig. 4I, CTA-paired group). This group of animals showed saccharin-induced freezing comparable with that of the control (CTA-unpaired) group in test 2 and test 5 without optical illumination. Original memories for either CTA (Fig. 4J) or AFC (Fig. 4K) were intact even under light illumination in test 3. When compared with the respective CTA- or AFC-unpaired group, the CTA- and AFC-paired groups showed comparable aversion indexes (Fig. 4J, test 2 and test 5, and fig. S7E), tone-induced freezing (fig. S7, A, B, D, and F), and saccharin-induced freezing (fig. S7C, test 2 and test 5) under no light illumination.

Our study reveals that repetitive coretrieval reorganizes two aversive memory traces to generate an intersectional neuronal ensemble, neurons shared by both prestored CTA and AFC memories. The overlapping ensemble is responsible for memory association but is dispensable for the retrieval of original memories. An increase in overlapping ensembles has been observed when memories are associated in a variety of learning paradigms (*4*, *12*–*14*, *24*, *25*). Moreover, memories for events occurring close together in time generate an interaction that accompanies an overlap in the cell ensembles of each memory (*13*, *14*). Memory trace is not always allocated at the primary active neurons and could be potentially reallocated to the different subsets of neuronal ensembles (*7*, *9*). The increase in the overlap between CTA and AFC ensembles suggests that the overlapping ensemble is newly formed by the RCS. Thus, after the RCS, CTA and AFC memory traces are reallocated and reorganized to form a memory linkage. Generating an overlapping neuronal ensemble is a general mechanism underlying a linkage between memories during both acquisition and retrieval. Our finding of an overlapping ensemble that is responsible for memory association but dispensable for retrieval of original memories may provide a way to dissociate daily memories that relate in some way to the circumstances of a trauma (*29*) from a traumatic event. This could help prevent flashback in individuals with posttraumatic stress disorder.

REFERENCES AND NOTES

1. D. O. Hebb, *The Organization of Behavior: A Neuropsychological Approach* (John Wiley and Sons, 1949).
2. J. R. Anderson, G. H. Bower, *Human Associative Memory* (Wiley, 1973).
3. T. Rogerson *et al*., *Nat. Rev. Neurosci.* **15**, 157–169 (2014).
4. M. Nomoto *et al*., *Nat. Commun.* **7**, 12319 (2016).
5. T. Takeuchi *et al*., *Nature* **537**, 357–362 (2016).
6. X. Liu *et al*., *Nature* **484**, 381–385 (2012).
7. S. A. Josselyn, S. Köhler, P. W. Frankland, *Nat. Rev. Neurosci.* **16**, 521–534 (2015).
8. S. Tonegawa, X. Liu, S. Ramirez, R. Redondo, *Neuron* **87**, 918–931 (2015).
9. A. Holtmaat, P. Caroni, *Nat. Neurosci.* **19**, 1553–1562 (2016).
10. A. R. Garner *et al*., *Science* **335**, 1513–1516 (2012).
11. S. Ramirez *et al*., *Science* **341**, 387–391 (2013).
12. N. Ohkawa *et al*., *Cell Rep.* **11**, 261–269 (2015).
13. D. J. Cai *et al*., *Nature* **534**, 115–118 (2016).
14. A. J. Rashid *et al*., *Science* **353**, 383–387 (2016).
15. Y. Zhou *et al*., *Nat. Neurosci.* **12**, 1438–1443 (2009).
16. K. Hashikawa *et al*., *J. Neurosci.* **33**, 4958–4963 (2013).
17. T. Inui, C. Inui-Yamamoto, Y. Yoshioka, I. Ohzawa, T. Shimura, *Neurobiol. Learn. Mem.* **106**, 210–220 (2013).
18. J. E. LeDoux, *Annu. Rev. Neurosci.* **23**, 155–184 (2000).
19. C. Herry *et al*., *Nature* **454**, 600–606 (2008).
20. G. Ferreira, M. I. Miranda, V. De la Cruz, C. J. Rodríguez-Ortiz, F. Bermúdez-Rattoni, *Eur. J. Neurosci.* **22**, 2596–2604 (2005).
21. J. Courtin *et al*., *Nature* **505**, 92–96 (2014).
22. J. Debiec, V. Doyère, K. Nader, J. E. Ledoux, *Proc. Natl. Acad. Sci. U.S.A.* **103**, 3428–3433 (2006).
23. A. Vazdarjanova, B. L. McNaughton, C. A. Barnes, P. F. Worley, J. F. Guzowski, *J. Neurosci.* **22**, 10067–10071 (2002).
24. S. K. Barot, Y. Kyono, E. W. Clark, I. L. Bernstein, *Proc. Natl. Acad. Sci. U.S.A.* **105**, 20959–20963 (2008).
25. Q. Yuan, J. S. Isaacson, M. Scanziani, *PLOS ONE* **6**, e20486 (2011).
26. L. G. Reijmers, B. L. Perkins, N. Matsuo, M. Mayford, *Science* **317**, 1230–1233 (2007).
27. R. Feil, J. Wagner, D. Metzger, P. Chambon, *Biochem. Biophys. Res. Commun.* **237**, 752–757 (1997).
28. T. Kawashima *et al*., *Nat. Methods* **10**, 889–895 (2013).
29. C. R. Brewin, E. A. Holmes, *Clin. Psychol. Rev.* **23**, 339–376 (2003).

ACKNOWLEDGMENTS

We thank K. Deisseroth (Stanford University) for the ArchT 3.0-EYFP cDNA, H. Hioki and T. Kaneko (Kyoto University) for the STB vector, and H. Bito (Tokyo University) for the E-SARE cDNA. All members of the Inokuchi laboratory supported and discussed this study. This work was supported by the CREST program of JST; Japan Society for the Promotion of Science KAKENHI grant numbers JP23220009 (K.I.), JP23650208, JP25293136 (F.K.), JP25430015 (A.M.W.), JP25860429, JP15K19194 (Y.T.), and 15K18344 (M. Nomoto); a Grant-in-Aid for Scientific Research on Innovative Areas "Memory dynamism" [JP25115002 (K.I.) and JP26115523 (A.M.W.)] and "Microendophenotypes of psychiatric disorders" [JP15H01295 (A.M.W.)] from the Ministry of Education, Culture, Sports, Science and Technology (MEXT); MEXT-Supported Program for the Strategic Research Foundation at Private Universities S1311009 (F.K.); the Mitsubishi Foundation; the Uehara Memorial Foundation; and the Takeda Science Foundation (support to K.I.). All data necessary to understand and assess the conclusions of this research are available in the supplementary materials.

SUPPLEMENTARY MATERIALS

www.sciencemag.org/content/355/6323/398/suppl/DC1
Materials and Methods
Figs. S1 to S8
Tables S1 and S2
References (*30*–*35*)
Data File S1

24 October 2016; accepted 4 January 2017
10.1126/science.aal2690

Overlapping memory trace indispensable for linking, but not recalling, individual memories

Jun Yokose, Reiko Okubo-Suzuki, Masanori Nomoto, Noriaki Ohkawa, Hirofumi Nishizono, Akinobu Suzuki, Mina Matsuo, Shuhei Tsujimura, Yukari Takahashi, Masashi Nagase, Ayako M. Watabe, Masakiyo Sasahara, Fusao Kato and Kaoru Inokuchi

Science **355** (6323), 398-403.
DOI: 10.1126/science.aal2690

Unrelated memories get blurred together

If one retrieves two memories around the same time, a small number of neurons will become involved in both memories. Yokose *et al.* investigated the cellular ensemble mechanisms underlying the association between two such memories. In mice, a small population of neurons mediates the association. Memory traces for two independent emotional memories in the brain partially overlapped when the two memories were retrieved synchronously to create a linkage. Suppressing the activity of the overlapping memory trace interrupted the linkage without damaging the original memories.

Science, this issue p. 398